CHEMISTRY
A EUROPEAN JOURNAL

DOI: 10.1002/chem.200801293

Space- and Time-Resolved In-situ Spectroscopy on the Coke Formation in Molecular Sieves: Methanol-to-Olefin Conversion over H-ZSM-5 and H-SAPO-34

Davide Mores,[a] Eli Stavitski,[a] Marianne H. F. Kox,[a] Jan Kornatowski,[b] Unni Olsbye,[c] and Bert M. Weckhuysen*[a]

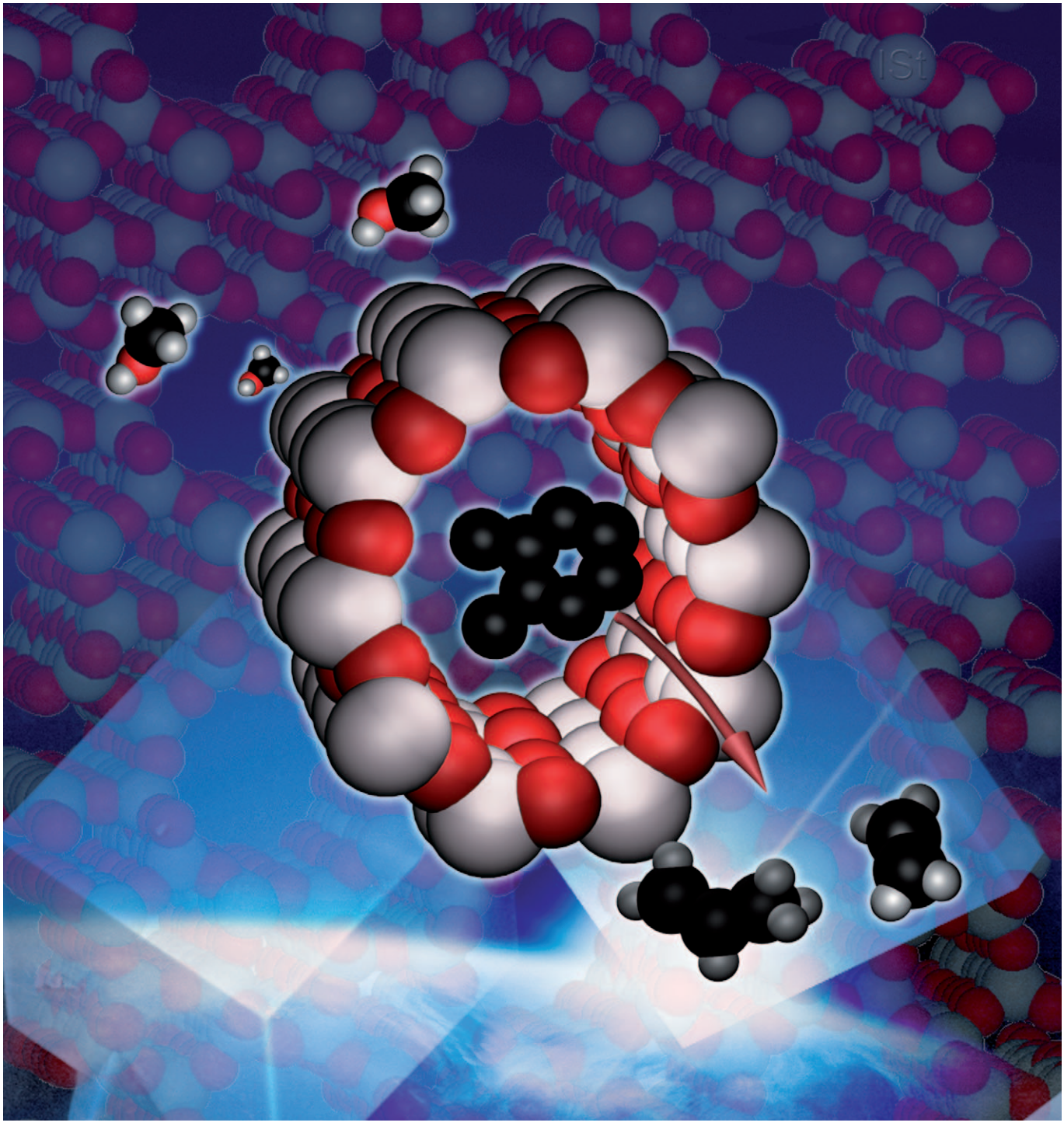

Abstract: Formation of coke in large H-ZSM-5 and H-SAPO-34 crystals during the methanol-to-olefin (MTO) reaction has been studied in a space- and time-resolved manner. This has been made possible by applying a high-temperature in-situ cell in combination with micro-spectroscopic techniques. The buildup of optically active carbonaceous species allows detection with UV/Vis microscopy, while a confocal fluorescence microscope in an upright configuration visualises the formation of coke molecules and their precursors inside the catalyst grains. In H-ZSM-5, coke is initially formed at the triangular crystal edges, in which straight channel openings reach directly the external crystal surface. At reaction temperatures ranging from 530 to 745 K, two absorption bands at around 415 and 550 nm were detected due to coke or its precursors. Confocal fluorescence microscopy reveals fluorescent carbonaceous species that initially form in the near-surface area and gradually diffuse inwards the crystal in which internal intergrowth boundaries hinder a facile penetration for the more bulky aromatic compounds. In the case of H-SAPO-34 crystals, an absorption band at around 400 nm arises during the reaction. This band grows in intensity with time and then decreases if the reaction is carried out between 530 and 575 K, whereas at higher temperatures its intensity remains steady with time on stream. Formation of the fluorescent species during the course of the reaction is limited to the near-surface region of the H-SAPO-34 crystals, thereby creating diffusion limitations for the coke front moving towards the middle of the crystal during the MTO reaction. The two applied micro-spectroscopic techniques introduced allow us to distinguish between graphite-like coke deposited on the external crystal surface and aromatic species formed inside the zeolite channels. The use of the methods can be extended to a wide variety of catalytic reactions and materials in which carbonaceous deposits are formed.

Keywords: coke · heterogeneous catalysis · methanol · microspectroscopy · zeolites

Introduction

The methanol-to-olefin (MTO) process, which is the selective transformation of methanol into light olefins, has attracted large interest from both academia and industrial scientists in view of the high demand for light olefins in the petrochemical industry.[1] Methanol is thereby regarded as an alternative raw material for crude oil that can be produced from syn-gas, a mixture of CO and H_2, which in turn, can be made from biomass, natural gas, or coal.[2] The most studied catalysts for the MTO reaction are H-SAPO-34 and H-ZSM-5.[1,3] The acidic centres of these materials are responsible for the chemical transformation of methanol into valuable hydrocarbons, while their pore architecture offers well-defined confined spaces, providing the desired product shape selectivity. However, independent of the catalytic properties, both molecular sieves deactivate with time-on-stream due to the formation of coke deposits, thereby affecting their potential application on an industrial scale.[1,3–5]

[a] D. Mores, Dr. E. Stavitski, M. H. F. Kox, Prof. Dr. Ir. B. M. Weckhuysen
Inorganic Chemistry and Catalysis Group
Department of Chemistry
Debye Institute for Nanomaterials Science, Utrecht University
Sorbonnelaan 16, 3584 CA Utrecht (The Netherlands)
Fax: (+31) 30-251-1027
E-mail: b.m.weckhuysen@uu.nl

[b] Dr. J. Kornatowski
Max-Plank-Institut für Kohlenforschung
45470 Mülheim an der Ruhr (Germany)
and
Faculty of Chemistry, Nicholas Copernicus University
87–100 Torun (Poland)

[c] Prof. U. Olsbye
Department of Chemistry, University of Oslo
0315 Oslo (Norway)

Architecturally, H-ZSM-5 has the MFI-type structure composed of straight channels (0.51 nm × 0.54 nm) and intersecting sinusoidal channels (0.54 nm × 0.56 nm). H-SAPO-34 molecular sieves on the other hand has a CHA-type structure, containing large cavities (0.65 nm × 1.1 nm) connected through narrow windows (0.42 nm × 0.37 nm).[6,7] In both molecular sieves, the conversion of methanol into hydrocarbons is believed to occur by the so-called hydrocarbon pool mechanism. According to this mechanism, the reaction takes place in a closed cycle in which methanol is initially converted into dimethyl ether (DME) and water. With the further addition of methanol, more water, as well as catalytic scaffolds, mainly composed of polymethyl-substituted benzene molecules, are formed. From these large organic molecules, alkenes are formed.[8–16] These intermediates do not only split-off the desired olefinic compounds, but can also react further, forming polyaromatic molecules and, eventually, graphitic coke.[17,18] It has been shown that even methylated naphtalenes, which contain two aromatic rings, give low alkene formation rates compared to methylated benzenes, and are therefore minor contributors to product formation.[19] Therefore, all compounds ranging from bi- and polyaromatic compounds to graphitic carbon will be denoted as "coke" in this contribution.

Coke compounds may adsorb on the acid sites, poisoning the catalyst active centres. In addition, coke formation leads to pore blocking, which restricts both the access of reactants towards the catalytic scaffold and the exit of products formed. Pore blocking in H-ZSM-5 zeolites has been related to the formation of polyaromatic compounds at the channel intersections or on the outer surface, while in H-SAPO-34 it arises from polyaromatic molecules formed in the large cavities. Both processes lead to catalyst deactivation.[4,15,20–22]

From the above discussions it is evident that differences in pore architecture affect the coke formation and therefore the activity of the catalyst. In this respect, H-ZSM-5, although less sensitive to deactivation as compared to H-SAPO-34, has a low selectivity towards light olefins. H-SAPO-34 exhibits 90% selectivity towards light olefins in the 623–698 K range. Furthermore, with increasing temperature (623–723 K), an enhanced selectivity towards ethene and propene is observed although combined with a faster deactivation.[23,24] However, coke formation may also affect the catalyst selectivity. During deactivation at a given temperature, the ethene-to-propene ratio is shifted towards ethene.[9,25] Two hypotheses have been proposed to explain this behaviour; the first is that a decrease in the free space in the zeolite cavities with rising coke content suppresses the formation of methyl benzenes with 5–6 methyl groups, thereby favouring ethene formation.[9] The second is that product diffusion out of the catalyst crystals is hindered by the coke molecules, thereby favouring ethene diffusion.[25]

The current contribution aims to elucidate the differences in coke formation during the MTO reaction between H-ZSM-5 and H-SAPO-34 molecular sieves by employing large crystals as model systems. By using in-situ UV/Vis micro-spectroscopy and confocal fluorescence microscopy, in conjunction with a high-temperature in-situ cell, we demonstrate that clear differences can be observed in the rate and patterning of the coke formation in a space- and time-resolved manner within the molecular-sieve crystals. The observed differences in coke formation behaviour will be explained in terms of the pore architecture and the intergrowth structure of both molecular sieves.

Results and Discussion

Figure 1 shows the scanning electron microscopy (SEM) images of the H-SAPO-34 ($50\times50\times50$ μm) and H-ZSM-5 ($100\times20\times20$ μm) crystals under study. It should be noted that these zeolite crystals are not single crystals and are composed of several intergrowth subunits, as has been recently elucidated (Figure 1b–d).[26,27] Zeolite crystals were placed on the heating stage of the in-situ cell, while exposed to a stream of methanol vapour at the reaction temperatures in the range of 530–745 K. During the reaction, the crystals were monitored using UV/Vis micro-spectroscopy and (confocal) fluorescence microscopy. In what follows, we will discuss these in-situ spectroscopy results separately for the H-ZSM-5 and H-SAPO-34 crystals.

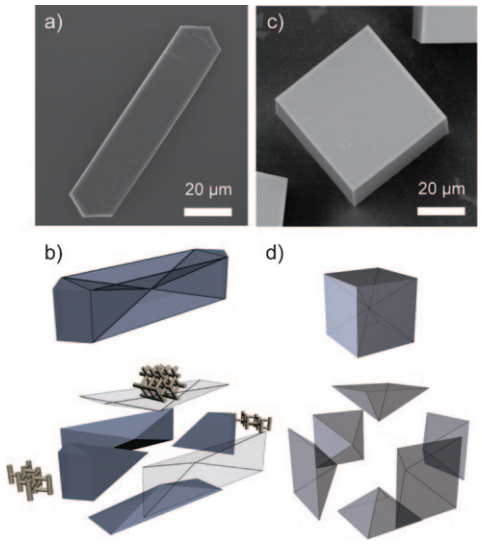

Figure 1. Scanning electron micrograph (SEM) pictures of the micron-sized H-ZSM-5 (a, b) and H-SAPO-34 (c, d) crystals under study together with the proposed intergrowth structures and the exploded representation thereof with pore orientation (b, d).

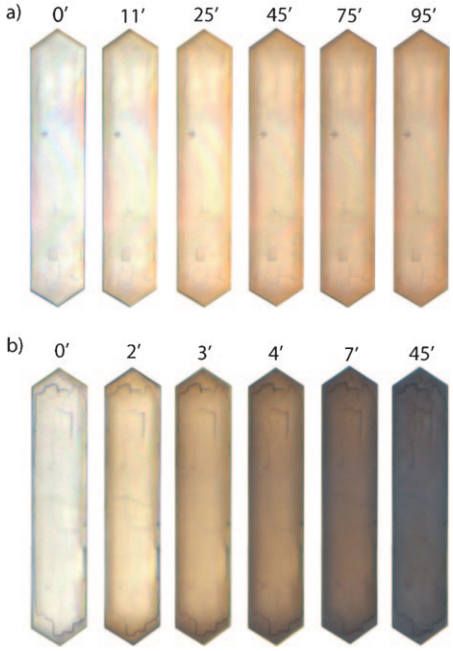

Figure 2. Optical microphotographs of H-ZSM-5 crystals taken during the MTO reaction at a) 530 K and b) 745 K. The corresponding time is indicated in minutes.

In-situ micro-spectroscopy study on the MTO reaction over H-ZSM-5 crystals: Upon exposure to methanol vapour, the translucent H-ZSM-5 crystals turn yellow-brown due to the formation of carbonaceous deposits. Figure 2 shows a selection of the optical micrographs of the H-ZSM-5 crystals taken during the MTO reaction as a function of time-on-stream at a reaction temperature of 530 and 745 K. From the inspection of Figure 2 we observe that the crystal coloration intensifies with reaction temperature. It is also worth noting that the coke deposition is faster on the triangular areas at the ends of the crystals during the early stage of the MTO reaction. It should be pointed out that according to the architecture of the H-ZSM-5 crystal intergrowth, as shown in Figure 1, the straight pores are open to the surface in these areas.[28]

With time-on-stream, the darkening spreads onto the central area of the H-ZSM-5 zeolite crystal. Moreover, the color of the crystal varies, depending on the reaction temperature, from brown to black. These color variations are reflected in the optical absorption measurements. Time-resolved optical absorption measurements taken from a 2 μm spot in the central region of the H-ZSM-5 crystals during the MTO reaction are shown in Figure 3. The optical spectra reveal two broad bands at 415 and 550 nm with their intensities increasing with increasing time-on-stream. In addition, a broad background absorption stretching across the whole visible region becomes apparent at high temperatures. The intensity of both bands directly correlates with the reaction temperature (Figure 3). The absorption band around 410 nm has been observed previously and assigned to the π–π* transitions in methyl-substituted benzenium cations.[15,29–37] These species play an important role in the hydrocarbon pool mechanism, by constituting the catalytic engine for alkene formation in interaction with the acidic centres of the zeolite.[13,38] As to the band at 550 nm, the red shift suggests that extended conjugated aromatic species originating from the benzenium species mentioned above are responsible for the optical absorption in this region. The observation that the latter absorption band formation lags behind the one at 415 nm (see Figure 3b) supports these assignments.[18,39]

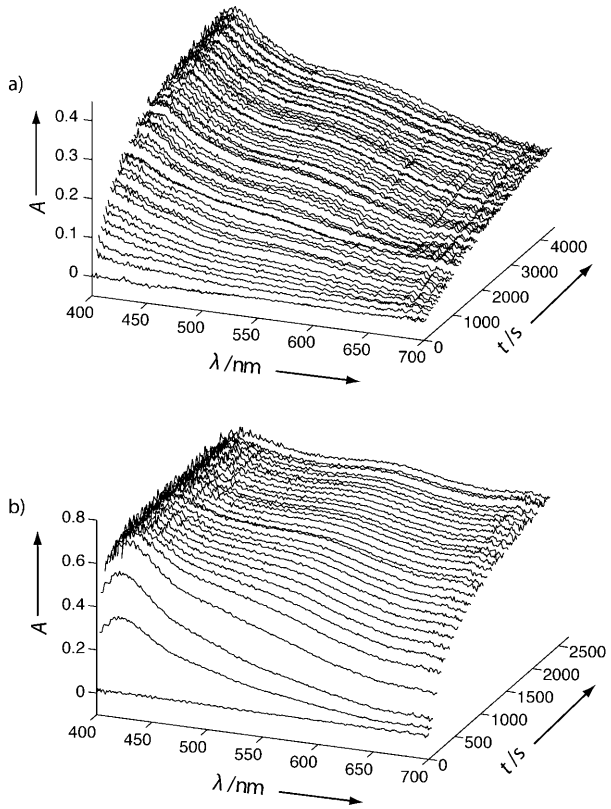

Figure 3. Optical absorption spectra of H-ZSM-5 crystals during the MTO reaction taken at a) 530 K and b) 745 K. The spectra were taken from a spot in the crystal centre.

The temporal evolution of the absorption band at ≈415 nm, as shown in Figure 4, allows the identification of two distinct temperature regions. Below 573 K, the profiles

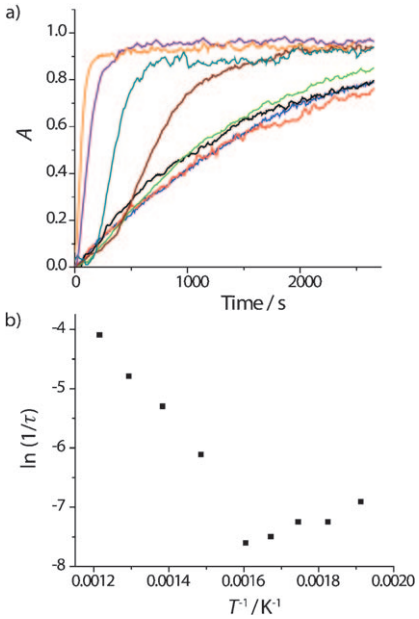

Figure 4. a) Temporal evolution of the optical absorption at 415 nm taken from a spot in the centre of the H-ZSM-5 crystal, as a function of time-on-stream for different reaction temperatures: 510 K (red); 530 K (black); 550 K (blue); 573 K (green); 615 K (wine); 660 K (cyan); 700 K (purple); 745 K (orange); b) Corresponding Arrhenius plot of the fitted curves shown in a).

remain identical within the experimental error, whereas above that point higher temperatures result in faster kinetics. This is emphasised by the Arrhenius plot of apparent reaction rate versus reaction temperature, as shown in Figure 4b. The reaction rates have been extracted from the time evolution profiles by fitting with first-order kinetics.[40]

The above-mentioned findings can be rationalised considering two different types of carbonaceous species produced during the MTO reaction. It has been shown for H-ZSM-5 catalysts that polymethylated benzenes, which participate in the catalytic cycle, are formed within zeolite channels, whereas graphite-like layers are deposited on the external surface of the crystal.[13,36,41] The latter is proposed to be responsible for the deactivation of H-ZSM-5, which is unique compared to the microporous materials with larger cavities, in which the coke is readily formed.[13,42] Along these lines, it is reasonable to assume that the aromatic compounds are responsible for the absorption band at 415 nm, while external graphite absorbs all the wavelengths across the optical region. Both species contribute to the apparent absorption at around 400 nm (Figure 3). At 530–573 K, aromatic compounds within zeolite channels are predominantly formed. This process appears to be nearly activationless, as evidenced in the low-temperature region of the Arrhenius plot. It is plausible that in those temperatures, the formation of

aromatic compounds is mainly dependent on the mass transport to the bulk of the H-ZSM-5 crystals. Above 575 K, graphite formation becomes significant, as reflected by the appearance of the structureless absorption spectrum (Figure 3b). Facilitated cracking of hydrocarbons on H-ZSM-5, leading to the formation of the graphite residues appears to have a positive activation energy as evident from the high temperature region of the Arrhenius plot (Figure 4b).

In-situ UV/Vis micro-spectroscopy gives valuable insights into the coke deposition on zeolite crystals. However, the thickness of the layer probed with this method greatly varies depending on the optical properties of the sample. We have recently demonstrated that the carbonaceous species, formed by oligomerisation of hydrocarbons in zeolite channels, exhibit strong fluorescence.[26] Therefore, the spatial distribution of these compounds within the catalyst particle can be mapped in three dimensions by using confocal fluorescence microscopy. This approach has been applied in the present work to allow for a better discrimination between surface and bulk hydrocarbon species. Figure 5 shows the confocal images of the H-ZSM-5 crystals taken during the reaction. Two excitation wavelengths were used, namely of 488 and 561 nm, with the fluorescence detection windows at 510–550 and 575–635 nm, respectively.

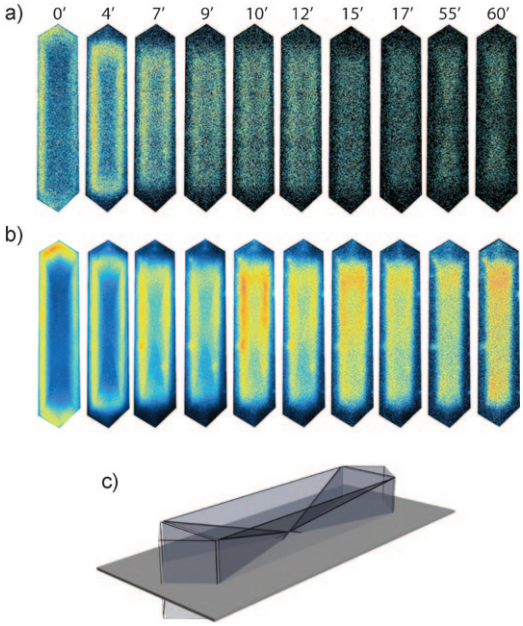

Figure 5. a) Fluorescence intensity profiles of H-ZSM-5 crystal during MTO reaction at 660 K depicted with time-on-stream at laser excitation a) 488 nm (detection at 510–550 nm) and b) 561 nm (detection at 565–635 nm). c) Schematic representation of the slice at which the confocal fluorescence measurement has been performed. The corresponding time is indicated in minutes.

Upon exposure to methanol, intense fluorescence is immediately observed at the near-surface region. With time-on-stream, both images exhibit a front of fluorescent molecules gradually moving from the crystal surface inwards. After ≈9 min of reaction, an hourglass pattern can be discerned in the images. This is due to the intracrystalline diffusion boundaries, arising at the subunits interfaces due to the mismatch of the channel orientation. As Figure 5 shows, fluorescent species photo-excited at 488 nm readily penetrate towards the inner core of the crystal compared to the compounds excited at 561 nm. It has been demonstrated by extraction experiments that restricted space in ZSM-5 channels inhibits formation of polyring aromatic compounds.[13] Therefore, the observed fluorescence is likely to be due to polymethylated benzene carbocations. The patterns obtained at varying excitation wavelengths are not identical, indicating that they correspond to distinct species, most likely, differing in their molecular dimensions. In the present case, it can be due to the different degree of methylation of the benzene ring. Alternatively, cations absorbing the shortest wavelengths may contain long conjugated chains that might exist within the 10-ring channels. Here, the red shift in the excitation wavelength indicates a larger molecular size. The observation that the species which exhibits fluorescence at lower wavelengths penetrates the intracrystalline boundaries faster supports this assumption.

With these findings, preferential accumulation of coke at the triangular edges of the crystals can be explained. The higher coloration intensity observed in these areas can in principle originate from intracrystalline hydrocarbon species or from the surface graphitic depositions. Confocal measurements supports the latter assumption, as no fluorescent intensity from those areas can be observed after ≈5 min of the reaction. This conclusion is fully consistent with the previous observations of spatially resolved reactivity of H-ZSM-5 crystals in the oligomerisation of styrene. Edge crystal regions appear to exhibit lower catalytic activity compared to the central area, hindering the growth of the styrene oligomeric chain.[43,44] These findings imply that the straight channels of H-ZSM-5 are more prone to pore blocking, whereas areas the channel system that are connected to the crystal surface through the segments of zigzag pores provide reactant and product molecules with more ways to diffuse inside and outside the crystal. In the present case, straight pore openings at the edges are blocked faster forcing the formation of the surface coke.

In-situ micro-spectroscopy study on the MTO reaction over H-SAPO-34 crystals: The SAPO-34 crystals have been investigated in a set of experiments similar to those for large H-ZSM-5 crystals described previously. In Figure 6, a selection of the optical microphotographs taken during the MTO reaction on H-SAPO-34 is shown. The images are depicted as a function of time-on-stream at two different reaction temperatures; that is, 530 and 745 K.

Comparison of Figures 2 and 6 reveals clear differences between the H-SAPO-34 and H-ZSM-5 crystals. For the reaction performed at 530 K, a strong yellow coloration has been observed along the edges of the crystals. Surprisingly, during the experiments, the colour intensity first strongly increases and later on decreases as illustrated by the image

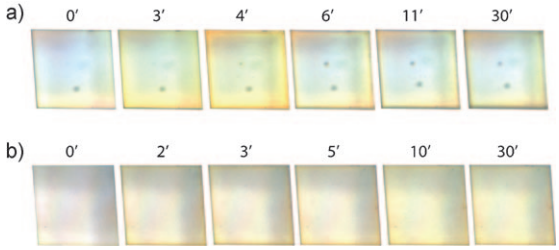

Figure 6. Optical microphotographs of H-SAPO-34 crystals taken during the MTO reaction at a) 530 K and b) 745 K. The corresponding time is indicated in minutes.

taken after 4 min in Figure 6a. However, such a drop was not observed above 573 K at which instead the crystals become darker and darker with time-on-stream.

The UV/Vis spectra of H-SAPO-34 crystal as a function of time-on-stream at a reaction temperature of 530 K is shown in Figure 7a. Similar to the case of the H-ZSM-5, the most prominent feature in the spectra is a strong absorption band at 400 nm, assigned to highly methyl-substituted benzene cations.[45–48] After reaching the intensity maximum, the absorption band decreases in intensity which is in line with the observed coloration. The time-resolved absorption measurements performed at 745 K, as summarised in Figure 7b, also show the formation of an absorption band at around 400 nm. However, the intensity of this absorption

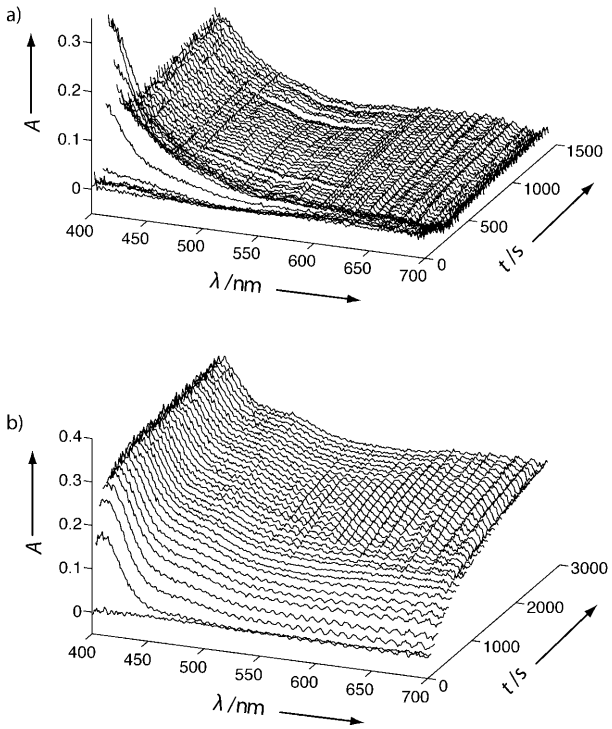

Figure 7. Diffuse reflectance UV/Vis spectra of H-SAPO-34 crystals during the MTO reaction as a function of time on stream at a) 530 K and b) 745 K. The spectra were taken from a spot in the middle of the crystal.

band does not decrease with time-on-stream. In addition, with increasing temperature, a second absorption band at 480 nm is formed. It should be noted that, as in the case of H-ZSM-5, the rise of this additional band does not occur at the expense of the 400 nm band. Furthermore, a rise of background over the whole spectrum is observed at elevated temperatures, indicating the formation of graphitic coke. In contrast to H-ZSM-5, however, no blackening was observed in the analysis of the optical microphotographs indicating that the carbonaceous deposits are mainly formed inside the H-SAPO-34 crystals.

Figure 8 shows the time evolution of the intensity of the absorption band at around 400 nm at different reaction temperatures as a function of time-on-stream. Similar to H-

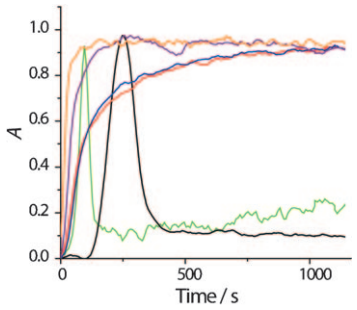

Figure 8. Time evolution of the optical absorption at 400 nm taken from a spot in the centre of the H-SAPO-34 crystal as a function of time-on-stream at different reaction temperatures:530 K (black); 573 K (green); 615 K (purple); 660 K (orange); 700 K (red); and 745 K (blue).

ZSM-5, two temperature regions can be discriminated. Below 573 K, the band intensity passes through a maximum and then drops to about 20% of its peak intensity. At higher temperatures, intensity of the band remains constant after reaching its maximal value. Remarkably, comparison of the kinetic profiles recorded at 615 K and above 700 K shows that the buildup of the 400 nm band is slower at higher temperatures.

It has been reported that, in contrast with H-ZSM-5, the reaction intermediates pool formed in H-SAPO-34 during the MTO process is not limited to mono-aromatic compounds.[10,15] This is due to the large cavities at the channel intersections, which can accommodate relatively large molecules and could explain the two-phase kinetics of the optical absorption band at 400 nm observed at lower temperatures. First, the appearance of the band is associated with polymethylated benzenes that rapidly interconvert into di- and tri-aromatic compounds, reflected by the drop in the band intensity. As in the case of H-ZSM-5, at higher temperatures two processes contribute to the optical absorption around 480 nm namely, formation of aromatic compounds and graphite-type coke. The latter is evident from the appearance of broad absorption background in the spectrum (Figure 7b). Slowing down the kinetics above 660 K is in agreement with previous observations of a shift from accumula-

tion of aromatics towards cracking into olefins at increasing temperatures[12,49,50]

Confocal fluorescence microscopy measurements, similar to those performed with H-ZSM-5 were carried out with the H-SAPO-34 crystals. A selection of the confocal fluorescence images taken is shown in Figure 9a, in which the resulting fluorescence intensity profiles recorded at 660 K using the 561 nm laser excitation are exhibited.

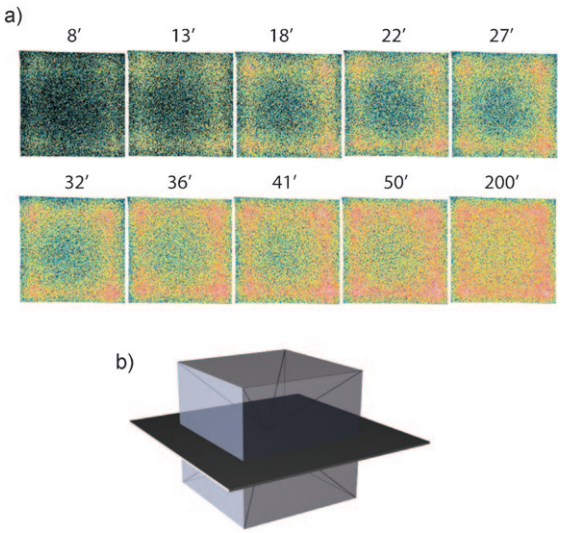

Figure 9. a) Confocal fluorescence intensity profiles of the H-SAPO-34 crystal during the MTO reaction at 660 K, as a function of time-on-stream. The laser excitation is 561 nm (detection at 565–635 nm, false colors). The corresponding time is indicated in minutes. b) Schematic representation of the slice at which the confocal fluorescence measurement is performed.

The fluorescent compounds are initially formed at the crystal corners. In these crystal regions, the flux of reactants and products is leading to the fastest formation of fluorescent coke precursor molecules. Further on, the formation of these fluorescent species extends to the edges of the crystals. With time-on-stream, the fluorescent molecules form a front that slowly moves towards the centre of the crystal; however the majority of the fluorescent compounds, remains located at the edge of the crystal. It is worth noting the differences with the H-ZSM-5 crystals, which is in line with the proposed deactivation mechanism for H-SAPO-34 catalysts that involves formation of the poly-aromatic compounds in the cavities, hindering diffusion through the crystal. This process leads to the channel blockage, making internal region of the crystals less accessible to the reactant molecules.

Conclusion

We have demonstrated, by using the methanol-to-olefin (MTO) process as probe reaction and large crystals of two distinct molecular sieves, that the combination of in-situ UV/Vis spectroscopy and confocal fluorescence micro-spectroscopy is a very valuable tool to probe coke deposits and their precursors during catalytic reactions. This has been made possible by using a high-temperature in-situ gas-flow cell and a fluorescence microscope, which is—in contrast to the recent work of Roeffaers and co-workers[51,52] on for example, the self-condensation of furfuryl alcohol—in an upright configuration thus avoiding the use of an immersion lens. The versatile methodology illustrates that the formation of coke during the MTO reaction on H-ZSM-5 crystals significantly differs from that on H-SAPO-34 crystals. Coke on H-ZSM-5 crystals is initially formed at the edges of the crystal at which straight pores are in contact with the crystal outer surface. The crystal coloration intensifies with reaction temperature. Temporal profiles of the absorption bands show two distinct temperature regions confirming the formation of the two distinctive coke systems, that is, methylated aromatic systems and graphitic coke compounds. The architecture of the H-ZSM-5 crystals explains these findings: hydrocarbon compounds in the pore intersections contribute to the internal coke formation as well as olefin production, while graphitic compounds block the pore openings at the external surface of the crystals. Confocal fluorescence experiments confirm that the preferred accumulation of coke at the crystal edges is due to graphitic deposits at the external surface of the catalytic crystal, while, with time-on-stream, a coke front composed of polymethylated aromatic species moves towards the centre of the catalytic crystal, while intracrystalline boundaries slow down the internal diffusion process. The H-SAPO-34 crystals show a fast formation of methyl-substituted aromatic compounds at the corners and edges of the catalyst crystal. With increasing temperature, larger coke compounds and graphitic deposits are formed. Confocal fluorescence measurements confirm the formation of fluorescent coke compounds starting at the corners of the H-SAPO-34 crystals, indicating that the majority of these species remains located at the edges of the crystal, thereby frustrating a further coke formation in the crystal core. These findings are also explained by the architecture of the crystal: large carbonaceous deposits formed in the cages at the edge of the crystal prevent the reaction front to move towards the centre of the crystal leading to fast catalyst deactivation.

Experimental Section

Materials and experiments: H-SAPO-34 crystals were prepared as reported elsewhere,[26] whereas large H-ZSM-5 crystallites were provided by ExxonMobil (Machelen, Belgium). The latter has been described in detail in our previous publications.[22,32,33] The Si/Al ratios of these crystals were 0.4 for H-SAPO-34 and 17 for H-ZSM-5 as determined by SEM-EDX and XRF measurements respectiveley. Methanol (Antonides-Interchema) was used as received. The experiments were performed in an appropriate in-situ cell (Linkam FTIR 600) equipped with a temperature controller (Linkam TMS 93). The calcined crystals were heated to 775 K at the rate of 10 K min^{-1} and kept at this temperature for 1 h under inert atmosphere. Subsequently, the temperature was brought to the required reaction temperature at the rate of 10 K min^{-1} after which the nitrogen flow was diverted through a bubbler containing a methanol solution thereby acting as carrier gas.

In-situ optical microscopy setup: An Olympus BX41 upright research microscope equipped with a 50×0.5 NA-high working distance objective was used. A 75 W tungsten lamp provided the illumination. The in-situ setup was equipped with a 50/50 double-viewport tube, that accommodates a CCD video camera (ColorView IIIu, Soft Imaging System GmbH) and an optical fibre mount. A 200 μm-core fibre connected the microscope to a CCD UV/Vis spectrometer (AvaSpec-2048TEC, Avantes).

In-situ confocal fluorescence microscopy setup: Fluorescence studies were performed on a Nikon Eclipse LV150 upright microscope with a 50×0.55 NA dry lens. The confocal fluorescence images were collected with the use of a Nikon D-Eclipse C1 head connected to the laser light sources (405, 488 and 561 nm). The emission was detected with two photomultiplier tubes in the 510–550 and 575–635 nm range.

Acknowledgements

This work was supported by the Dutch National Science Foundation (NWO-CW VICI and TOP subsidies to B.M.W. and VENI subsidy to E.S.) and the National Research School Combination Catalysis (NRSC-C). Dr. Machteld Mertens (ExxonMobil, Belgium) is acknowledged for providing the ZSM-5 crystals. Marjan Versluijs-Helder is acknowledged for performing the SEM-EDX and XRF measurements.

[1] M. Stöcker, *Microporous Mesoporous Mater.* **1999**, *29*, 3.
[2] G. A. Olah, *Angew. Chem.* **2005**, *117*, 2692; *Angew. Chem. Int. Ed.* **2005**, *44*, 2636.
[3] G. F. Froment, W. J. H. Dehartog, A. J. Marchi, *Catalysis* **1992**, *9*, 1.
[4] D. M. Bibby, R. F. Howe, G. D. McLellan, *Appl. Catal. A* **1992**, *93*, 1.
[5] H. van Bekkum, E. M. Flaningen, P. A. Jacobs, J. C. Jansen, *Introduction to Zeolite Science & Practice*, Elsevier, Amsterdam, **2001**.
[6] C. Baerlocher, W. M. Meier, D. H. Olson, *Atlas of Zeolite Framework Types*, Elsevier, Amsterdam, **2001**.
[7] See: www.iza-structure.org/database.
[8] H. Fu, W. G. Song, J. F. Haw, *Catal. Lett.* **2001**, *76*, 89.
[9] W. G. Song, H. Fu, J. F. Haw, *J. Am. Chem. Soc.* **2001**, *123*, 4749.
[10] J. F. Haw, W. G. Song, D. M. Marcus, J. B. Nicholas, *Acc. Chem. Res.* **2003**, *36*, 317.
[11] B. Arstad, J. B. Nicholas, J. F. Haw, *J. Am. Chem. Soc.* **2004**, *126*, 2991.
[12] M. Bjorgen, U. Olsbye, D. Petersen, S. Kolboe, *J. Catal.* **2004**, *221*, 1.
[13] U. Olsbye, M. Bjorgen, S. Svelle, K. P. Lillerud, S. Kolboe, *Catal. Today* **2005**, *106*, 108.
[14] S. Svelle, F. Joensen, J. Nerlov, U. Olsbye, K. P. Lillerud, S. Kolboe, M. Bjorgen, *J. Am. Chem. Soc.* **2006**, *128*, 14770.
[15] M. Bjorgen, S. Svelle, F. Joensen, J. Nerlov, S. Kolboe, F. Bonino, L. Palumbo, S. Bordiga, U. Olsbye, *J. Catal.* **2007**, *249*, 195.
[16] C. Arcangeli, S. Cannistraro, *Biopolymers* **2000**, *57*, 179.
[17] J. F. Haw, D. M. Marcus, *Top. Catal.* **2005**, *34*, 41.
[18] M. Bjørgen, U. Olsbye, S. Kolboe, *J. Catal.* **2003**, *215*, 30.
[19] W. G. Song, H. Fu, J. F. Haw, *J. Phys. Chem. B* **2001**, *105*, 12839.
[20] A. T. Aguayo, A. E. S. del Campo, A. G. Gayubo, A. Tarrio, J. Bilbao, *J. Chem. Technol. Biotechnol.* **1999**, *74*, 315.
[21] D. Chen, H. P. Rebo, K. Moljord, A. Holmen, *Ind. Eng. Chem. Res.* **1997**, *36*, 3473.
[22] D. Chen, H. P. Rebo, K. Moljord, A. Holmen, *Ind. Eng. Chem. Res.* **1999**, *38*, 4241.
[23] D. Chen, K. Moljord, T. Fuglerud, A. Holmen, *Microporous Mesoporous Mater.* **1999**, *29*, 191.
[24] J. Liang, H. Li, W. Guo, R. Wang, M. Ying, *Appl. Catal.* **1990**, *64*, 31.
[25] P. Barger, *Zeolites for Cleaner Technologies*, Imperial College Press, London, **2002**.
[26] L. Karwacki, E. Stavitski, M. H. F. Kox, J. Kornatowski, B. M. Weckhuysen, *Angew. Chem.* **2007**, *119*, 7366; *Angew. Chem. Int. Ed.* **2007**, *46*, 7228.
[27] E. Stavitski, M. R. Drury, D. A. M. de Winter, M. H. F. Kox, B. M. Weckhuysen, *Angew. Chem.* **2008**, *120*, 5719; *Angew. Chem. Int. Ed.* **2008**, *47*, 5637.
[28] M. H. F. Kox, E. Stavitski, J. C. Groen, J. Pérez-Ramírez, F. Kapteijn, B. M. Weckhuysen, *Chem. Eur. J.* **2008**, *14*, 1718.
[29] J. Melsheimer, D. Ziegler, *J. Chem. Soc. Faraday Trans.* **1992**, *88*, 2101.
[30] M. Bjorgen, U. Olsbye, S. Svelle, S. Kolboe, *Catal. Lett.* **2004**, *93*, 37.
[31] Y. J. Jiang, M. Hunger, W. Wang, *J. Am. Chem. Soc.* **2006**, *128*, 11679.
[32] W. Wang, Y. J. Jiang, M. Hunger, *Catal. Today* **2006**, *113*, 102.
[33] I. Kiricsi, H. Forster, G. Tasi, J. B. Nagy, *Chem. Rev.* **1999**, *99*, 2085.
[34] M. Bjorgen, F. Bonino, S. Kolboe, K. P. Lillerud, A. Zecchina, S. Bordiga, *J. Am. Chem. Soc.* **2003**, *125*, 15863.
[35] M. Bjørgen, F. Bonino, B. Arstad, S. Kolboe, K. P. Lillerud, A. Zecchina, S. Bordiga, *ChemPhysChem* **2005**, *6*, 232.
[36] L. Palumbo, F. Bonino, P. Beato, M. Bjorgen, A. Zecchina, S. Bordiga, *J. Phys. Chem. C* **2008**, *112*, 9710, and references therein.
[37] D. M. McCann, D. Lesthaeghe, P. W. Kletnieks, D. R. Guenther, M. J. Hayman, V. Van Speybroeck, M. Waroquier, J. F. Haw, *Angew. Chem.* **2008**, *120*, 5257; *Angew. Chem. Int. Ed.* **2008**, *47*, 5179.
[38] H. Forster, J. Seebode, P. Fejes, I. Kirisci, *J. Chem. Soc. Faraday Trans.* **1987**, *83*, 1109.
[39] A. Sassi, M. A. Wildman, J. F. Haw, *J. Phys. Chem. B* **2002**, *106*, 8768.
[40] Fitting the profile using second-order kinetics has also been attempted; however, using first-order kinetics represented the profiles more accurately for all different reaction temperatures tested.
[41] D. Chen, A. Gronvold, H. P. Rebo, K. Moljord, A. Holmen, *Appl. Catal. A* **1996**, *137*, L1.
[42] S. Gomm, R. Glaser, J. Weitkamp, *Chem. Eng. Technol.* **2002**, *25*, 962.
[43] M. H. F. Kox, E. Stavitski, B. M. Weckhuysen, *Angew. Chem.* **2007**, *119*, 3726; *Angew. Chem. Int. Ed.* **2007**, *46*, 3652.
[44] E. Stavitski, M. H. F. Kox, B. M. Weckhuysen, *Chem. Eur. J.* **2007**, *13*, 7057.
[45] J. Li, G. Xiong, Z. Feng, Z. Liu, Q. Xin, C. Li, *Microporous Mesoporous Mater.* **2000**, *39*, 275.
[46] W. G. Song, J. B. Nicholas, J. F. Haw, *J. Phys. Chem. B* **2001**, *105*, 4317.
[47] Y. J. Jiang, J. Huang, V. R. R. Marthala, Y. S. Ooi, J. Weitkamp, M. Hunger, *Microporous Mesoporous Mater.* **2007**, *105*, 132.
[48] Y. J. Jiang, W. Wang, V. R. R. Marthala, J. Huang, B. Sulikowski, M. Hunger, *J. Catal.* **2006**, *244*, 134.
[49] M. W. Anderson, B. Sulikowski, P. J. Barrie, J. Klinowski, *J. Phys. Chem.* **1990**, *94*, 2730.
[50] A. N. R. Bos, P. J. J. Tromp, H. N. Akse, *Ind. Eng. Chem. Res.* **1995**, *34*, 3808.
[51] M. B. J. Roeffaers, B. F. Sels, H. Uji-i, B. Blanpain, P. L'hoëst, P. A. Jacobs, F. C. De Schryver, J. Hofkens, D. E. De Vos, *Angew. Chem.* **2007**, *119*, 1736; *Angew. Chem. Int. Ed.* **2007**, *46*, 1706.
[52] M. B. J. Roeffaers, G. De Cremer, H. Uji-i, B. Muls, B. F. Sels, P. A. Jacobs, F. C. De Schryver, D. E. De Vos, J. Hofkens, *Proc. Natl. Acad. Sci. USA* **2007**, *104*, 12603.

Received: June 27, 2008
Published online: November 19, 2008

